ELSEVIER

Polymer 41 (2000) 1395–1407

polymer

# Nano-structured polymer blends: phase structure, crystallisation behaviour and semi-crystalline morphology of phase separated binary blends of poly(ethylene oxide) and poly(ether sulphone)

G. Dreezen[a], D.A. Ivanov[b], B. Nysten[c], G. Groeninckx[a,*]

[a]*Catholic University of Leuven (KULeuven), Department of Chemistry, Laboratory of Macromolecular Structural Chemistry, Celestijnenlaan 200F, B-3001 Heverlee, Belgium*

[b]*Université Libre de Bruxelles, Département de Physique, Unité de Physique des Polymères, CP 223, Boulevard du Triomphe, 1050 Brussels, Belgium*

[c]*Université Catholique de Louvain, Unité de Physique et de Chimie des Hauts Polymères, place croix du Sud, B-1348 Louvain-la-Neuve, Belgium*

Received 1 January 1999; received in revised form 30 March 1999; accepted 8 April 1999

**Abstract**

The crystallisation behaviour and morphology of binary phase separated crystalline/amorphous blends of poly(ethylene oxide) (PEO) and poly(ether sulphone) (PES) are investigated. The crystallisation behaviour of the PEO/PES blends changes strongly with demixing time and temperature. A method is proposed to determine the composition and amount of PEO-rich phase in the partially demixed blend systems from the dynamic crystallisation behaviour. The results are in agreement with the structure development as predicted for spinodal decomposition that proves the validity of this method. The phase and semi-crystalline morphologies are visualised by scanning electron microscopy and atomic force microscopy. The semi-crystalline morphology is also studied by real-time small angle and wide angle X-ray scattering. It is shown that, depending on the blend composition, a spherulitic or isolated lamellar crystalline morphology is formed in the demixed PEO/PES blends. 

*Keywords*: Nano-structures; PEO/PES blend; Crystallisation behaviour

## 1. Introduction

Structure formation in binary partially miscible polymer blends occurring from the combination of liquid–solid (crystallisation) and liquid–liquid phase separation is a research domain of growing interest in polymer science. This interest arises from the ability to develop various nano-structures by thermal treatment of the initially miscible polymer blend. Depending on the blend characteristics, phase separation and crystallisation can appear either in the same or in two different temperature regions. To control the final morphology in these blend systems, a thorough insight is needed in the phase separation and crystallisation behaviour, as well as in the semi-crystalline structure development. Moreover, this approach combining both phase separation and crystallisation can have a larger scope and is applicable to in-situ polymerisation and curing of polymer systems as well.

Tanaka and Nishi [1,2] were the first to introduce the concept of structure formation by combination of phase separation and crystallisation. Blends of poly(caprolactam) and poly(styrene) showing an upper critical solution temperature (UCST) type demixing were extensively investigated in the past [1–4]. Most of the investigated blend systems like polycarbonate/poly(butylene terephtalate) [5], polypropylene/ethylene-propylene copolymer [6], poly($\epsilon$-caprolactone)/poly(styrene-acrylonitrile) [7] or isotactic poly(propylene)/isotactic poly(1-butene) [8] concern low molecular weight polymers showing an UCST-type demixing [9–11]. Most of the partially miscible polymer blends consisting of high molecular weight components show a lower critical solution temperature (LCST) type [12,13].

Binary blends of a crystallizable component poly(ethylene oxide) (PEO) and an amorphous component poly(ether sulphone) (PES) are completely miscible up to 75°C and show a LCST-type demixing at higher temperatures. As a consequence, phase separation occurs at temperatures above the melting point of PEO (65°C). The phase behaviour, kinetics and thermodynamics of phase separation of these PEO/PES blends have been investigated in the past [14–16]. Very recently, the crystallisation and melting behaviour and the semi-crystalline morphology of miscible PEO/PES blends were studied [17,18].

In the present paper, the phase separation kinetics, the

* Corresponding author.

0032-3861/00/$ - see front matter 
PII: S0032-3861(99)00296-7

crystallisation behaviour after phase separation and possible remixing of the phase separated PEO/PES blends are reported. Further, the semi-crystalline morphology and phase morphology resulting from demixing and crystallisation are also considered. A method is proposed in order to determine the composition and amount of the PEO-rich phase present after phase separation.

## 2. Experimental

### 2.1. Materials and blend preparation

Poly(ethylene oxide) obtained from UCB (Belgium) with a viscosity average molecular weight ($\bar{M}_v$) of 17 000 g/mol and a polydispersity of 1.35 was blended with poly(ether sulphone) (trade name Victrex 4800G) obtained from Victrex Limited (UK) with a viscosity average molecular weight ($\bar{M}_v$) of 61 000 g/mol and a polydispersity of 1.72. Molecular weights of both components were determined by GPC-analysis on a Waters-instrument with dimethylformamide (DMF) as solvent. The glass-transition temperatures of PEO and PES are −65 and 225°C, respectively. PEO/PES blends of 75/25 and 50/50 (wt./wt.) compositions were prepared by solution blending in 10% (wt./vol.) DMF solutions. The blends were dried under vacuum at 70°C; additional drying was performed for 2 days at 60°C under vacuum. The 75/25 and 50/50 PEO/PES blend compositions were selected on the basis of the pronounced difference in their crystallisation behaviour.

### 2.2. Differential scanning calorimetry

A Perkin–Elmer DSC7 differential scanning calorimeter was used to investigate the crystallisation behaviour. The temperature and enthalpy calibrations were performed using benzophenone and indium standards. Experiments were performed under nitrogen atmosphere. Empty pan measurement was employed as a baseline correction. A typical thermal treatment of blend samples included melting in the miscible state for 5 min, phase separation at a higher temperature ($T_d$) and DSC-quenching to a temperature from which a DSC-ramp at −10°C/min was started. Different phase separation temperatures ($T_d$) and times ($t_d$) were used in this study. The 75/25 and 50/50PEO/PES blends were melted at 70 and 80°C, respectively. The DSC-measurements were started from the same temperatures. In some experiments, an additional step was included in the temperature program in order to remix the phase-separated blend. Different remixing temperatures ($T_r$) and times ($t_r$) were applied to both 75/25 and 50/50 PEO/PES blends. All mentioned crystallisation temperatures correspond to the peak temperature of the crystallisation exotherm. The degree of crystallinity is obtained by dividing the crystallisation enthalpy by the enthalpy of fusion of 100% crystalline PEO (i.e. 196.4 J/g) [19,20]. This value is normalised for the weight fraction PEO in the PEO/PES blend

$$X_c = \frac{\Delta H_{exp}}{196.4(\text{fraction}_{PEO})}. \quad (1)$$

### 2.3. Real-time small angle and wide angle X-ray scattering

Synchrotron radiation X-ray scattering experiments were carried out on the double focussing camera X33 [21] of the EMBL in HASYLAB on the storage ring DORIS III of the Deutches Elektronen Synchrotron (DESY) at Hamburg using a wavelength of 1.5 Å. Samples with a thickness of 1 mm were sealed between thin aluminum foils. Small angle X-ray scattering (SAXS) and wide angle X-ray diffraction (WAXD) patterns were simultaneously collected using gas proportional detectors [22] every 12 s during a thermal treatment similar to the DSC measurements (i.e. 1 pattern/2°C during cooling at −10°C/min). The temperature program was maintained using a Mettler Toledo FP82 hot stage mounted in the X-ray beam path. The WAXD detector was calibrated using benzoic acid and covered the *s*-range between 0.13 and 0.40 $Å^{-1}$, *s* being equal to

$$s = \frac{1}{\lambda}(2 \sin \theta) \quad (2)$$

where $2\theta$ is the scattering angle and $\lambda$ the wavelength.

The distance between the sample and the SAXS linear position sensitive detector was 400 cm. The SAXS detector was calibrated using rat tail collagen and covered the *s*-range between 0.0016 and 0.028 $Å^{-1}$. The SAXS and WAXD intensity curves were normalised to the primary X-ray beam intensity using the signal of an ionisation chamber placed in front of the sample. The SAXS-data were corrected for parasitic scattering by subtraction of an empty cell scattering. The curves were finally Lorentz corrected with a factor $s^2$ applicable for lamellar or plate-like systems [23]. The long period *L* was calculated from the position of the maximum in the Lorentz-corrected SAXS spectra. The invariant, or total scattering power, *Q* is obtained by integration of the Lorentz-corrected spectra:

$$Q = \int I(s)s^2 \, ds. \quad (3)$$

### 2.4. Optical microscopy

Cloud points were detected from the light transmitted by thin samples between glass slides under an OLYMPUS BH-2 optical microscope coupled with a computer controlled CCD-camera. The PEO/PES blend samples were heated at 1°C/min and the first decrease in transmitted light intensity was taken as the cloud point temperature. The same device equipped with a photo camera was used to obtain polarised optical micrographs of crystallised, phase-separated samples after a thermal treatment similar to the DSC experiments.

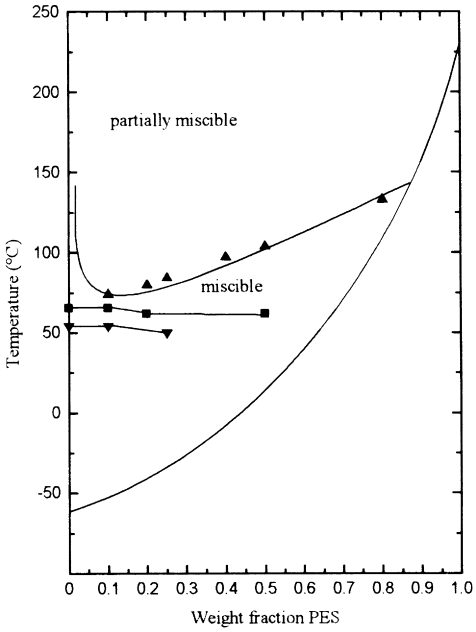


Fig. 1. Phase diagram of PEO/PES blends: (▲) cloud point curve, (■) melting temperature $T_m$, (▼) upper isothermal crystallisation temperature $T_c$, (—) glass-transition temperature $T_g$.

### 2.5. Scanning electron microscopy

Scanning electron micrographs were taken using a Philips XL-20 scanning electron microscope at an accelerating voltage of 20 kV. The sample preparation procedure included cold fracturing, etching in a 10% ethanol solution of sodium ethoxide [24] and gold coating. While pure PEO dissolves very fast in the etching solvent, PES is not soluble in it. Similar to PES, neither 50/50 nor 75/25 miscible PEO/PES blends dissolve in the etching solvent. The etching was performed during 12 min for the study of the semi-crystalline morphology (AFM) and 3 h for the study of the phase separated blend morphology (SEM). Field emission gun scanning electron microscopy (FEG-SEM) measurements were performed with a DSM 982 Gemini microscope operated at 1 kV.

### 2.6. Atomic force microscopy

AFM measurements of PEO/PES blends were performed with an Autoprobe CP (Park Scientific Instruments, Sunnyvale, CA) and a PicoSPM (Molecular Imaging, Phoenix, AZ) instrument under ambient conditions. All the measurements were made with 0.6 μm thick silicon nitride cantilevers ($kc \sim 0.3\ \mathrm{Nm}^{-1}$) in contact mode. The smallest value of contact force sufficient to produce a stable image was each time chosen for scanning (1–5 nN). Since blend samples were prepared from bulk specimens, their surface at large-scale is very rough with steep slopes resulting from cold fracturing. This type of sample topography is very difficult to image at large-scale due to the limited vertical motion of the piezoelectric scanner (~7 μm) and due to possible contacts of sharp and steep surface features with the cantilever rather than with the tip. Therefore, special care had to be taken to avoid possible artefacts of imaging. During the experiments, the same sample area was repetitively imaged varying the image size, the value of the applied force and the scanning direction. In order to exclude the possible influence of capillary forces acting on the surface of the hygroscope PEO-rich phase, some experiments were carried out under heptane.

## 3. Results and discussion

The aim of this paper is to describe the phase morphology and crystalline structure development in partially miscible blends of PEO and PES. The crystallisation behaviour of PEO in phase separated 75/25 and 50/50 PEO/PES blends has been investigated. From the crystallisation data, it was possible to determine the amount and composition of the PEO-rich phase. The phase morphology of the phase separated PEO/PES blends in which crystallisation occurs, and the resulting semi-crystalline morphology have also been studied.

PEO/PES blends exhibit a temperature and composition dependent miscibility; the corresponding phase diagram is presented in Fig. 1. The blends show an LCST-type phase diagram with a minimum at a 90/10 PEO/PES composition. They are miscible over the whole composition range below 75°C. The cloud point temperatures of the 75/25 and 50/50 PEO/PES blends are 80 and 101°C, respectively. The glass-transition temperature $T_g$ of the fully amorphous blends were estimated from the Fox-equation [25].

### 3.1. Crystallisation behaviour of demixed PEO/PES blends

The study of the crystallisation behaviour of PEO/PES blends in the miscible state revealed that a strong retardation of the crystallisation kinetics of PEO with an increasing amount of the amorphous component PES [17]. It was reported that a higher degree of undercooling was required for the crystallisation to start and that the spherulite growth rate decreased strongly when blending PEO with PES. During phase separation, a two-phase system is formed where each phase contains both components in different compositions. It is expected that the crystallisation behaviour of PEO/PES blends in the phase-separated state will strongly differ from that in the miscible state. Crystallisation of the PEO/PES blends has been investigated as a function of demixing temperature and time, and as a function of remixing temperature and time.

#### 3.1.1. Influence of demixing temperature

Firstly, the influence of the demixing temperature ($T_d$) on the crystallisation behaviour of phase separated PEO/PES blends is studied. The 75/25 and 50/50 PEO/PES blends were phase separated for 15 min at different temperatures and subsequently dynamically crystallised; the DSC-traces

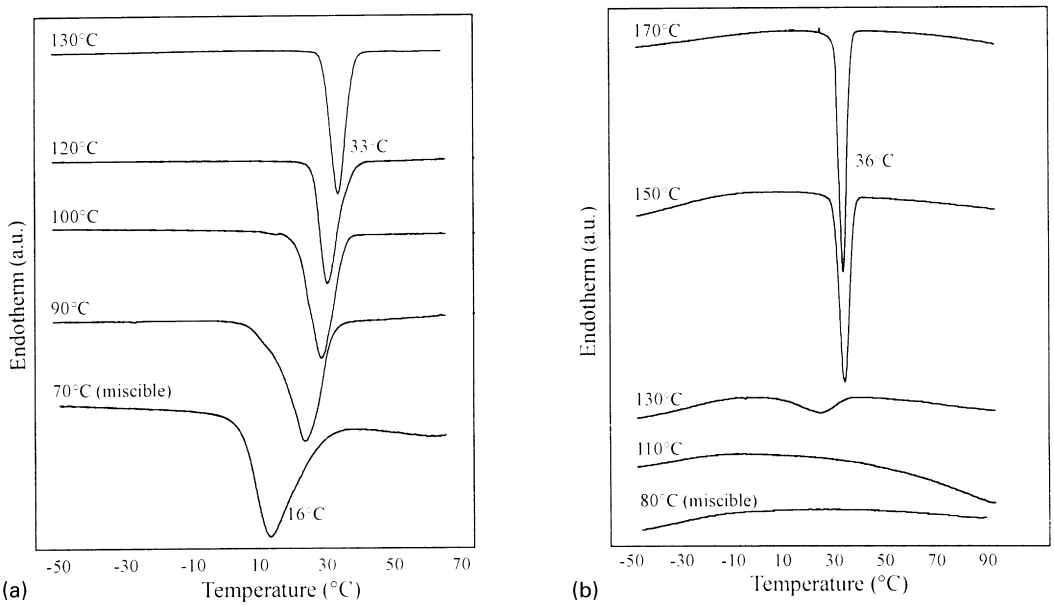


Fig. 2. DSC cooling curves of: (a) 75/25 and (b) 50/50 PEO/PES blends, phase separated for 15 min at different temperatures (indicated left of the curve).

are presented in Fig. 2. The 75/25 PEO/PES blend in the miscible state crystallises at 16°C. A clear shift to higher temperatures of the crystallisation exotherm of phase separated blends with increasing $T_d$ is observed (Fig. 2(a)). The 50/50 PEO/PES blend in the miscible state remains amorphous when cooled down from the melt (Fig. 2(b)). The 50/50 PEO/PES blend already shows a small crystallisation exotherm after demixing at $T_d = 130$°C; with increasing phase separation temperature, the crystallisation enthalpy increases and the peak shifts towards higher temperatures and becomes narrower.

The change of the PEO-crystallisation behaviour in the 75/25 and 50/50 PEO/PES blends with increasing $T_d$ is related to the formation of a two-phase system consisting of a PEO-rich phase and a PEO-poor phase. The shift of the crystallisation peak to higher temperatures signifies that crystallisation of PEO within the PEO-rich phase occurs faster than in the blend from the completely miscible state. This can be explained by the increased mobility of PEO in the PEO-rich phase. Moreover, the faster crystallisation in the phase-separated blends is also revealed in a narrowing of the crystallisation exotherm. From the absence

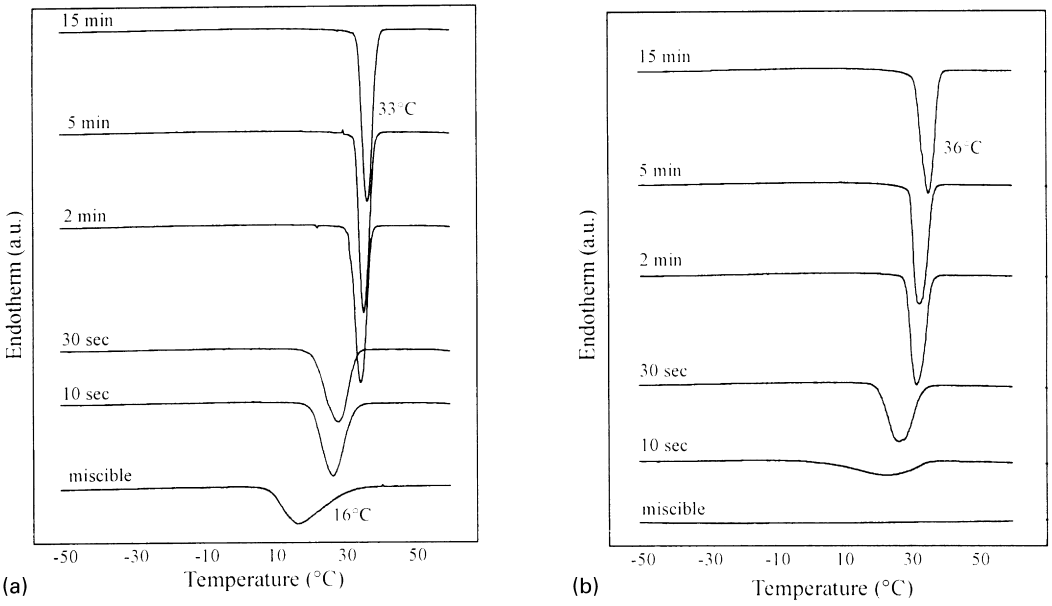


Fig. 3. DSC cooling curves of: (a) 75/25 PEO/PES blends isothermally demixed at 130°C and (b) 50/50 PEO/PES blends isothermally demixed at 150°C, after different demixing times (indicated left of the curve).

Table 1
Crystallinity of 75/25 and 50/50 PEO/PES blends determined after different thermal treatments

| PEO/PES blend composition (wt./wt.) | Thermal treatment | Degree of crystallinity (%) |
|---|---|---|
| 75/25 | Miscible | 60 |
| | 5 min, 130°C | 71 |
| | 15 min, 130°C | 72 |
| | 5 min, 130°C; 10 min, 75°C | 64 |
| 50/50 | Miscible | 0 |
| | 5 min, 150°C | 63 |
| | 15 min, 150°C | 65 |
| | 5 min, 150°C; 10 min, 95°C | 2 |

of an additional crystallisation exotherm, it can be concluded that the PEO-poor phase remains amorphous. This is attributed to the decreased mobility and increased $T_g$ of the PEO-poor phase compared to the PEO-rich phase.

### 3.1.2. Influence of demixing time

Besides the effect of the demixing temperature ($T_d$), the influence of the demixing time ($t_d$) on the crystallisation behaviour has also been studied. The DSC cooling traces of 75/25 and 50/50 PEO/PES blends after isothermal phase separation as a function of time at 130 and 150°C, respectively, are shown in Fig. 3. The crystallisation exotherm shifts to higher temperatures and narrows with increasing $t_d$ due to the decreased amount of PES in the PEO-rich phase that is the only phase able to crystallise. Within 5 min both blend compositions show a sharp crystallisation peak around 35°C. The crystallinity for the 75/25 PEO/PES blends changes from 60% in the miscible state up to 72% after phase separation ($t_d = 15$ min, $T_d = 130$°C), as summarised in Table 1. The crystallinity in the 50/50 PEO/PES blends changes from zero in the miscible state to 65% after demixing. Thus, the composition of the PEO-rich phase changes continuously during the phase separation process and accounts for the increase of crystallinity and crystallisation temperature.

### 3.1.3. Influence of remixing time

Thermodynamically, remixing or homogenisation occurs when a phase separated polymer blend is brought to the miscible temperature–composition region of the phase diagram. During dynamic crystallisation of phase separated PEO/PES blends this temperature region is passed on cooling. Thus it is necessary to study the extent of the remixing process and its influence on the crystallisation of the phase separated blends.

In these experiments, the 75/25 PEO/PES blend was demixed for 15 min at 130°C and kept isothermally at 70°C (10°C below the cloud point); the 50/50 PEO/PES blend was demixed for 15 min at 150°C and kept isothermally at 90°C. DSC-thermograms after different remixing times ($t_r$) of the 75/25 and 50/50 PEO/PES blends are presented in Fig. 4. The crystallisation exotherm of the 50/50 PEO/PES blend shifts to lower temperatures and broadens; after 30 min remixing time no crystallisation peak is present anymore. The change of the crystallisation behaviour indicates that the 50/50 PEO/PES blend remixes on the molecular level. However, the extent of remixing of a partially phase separated PEO/PES blend cannot be determined only from dynamic crystallisation experiments. PEO/PES blends in the miscible state containing more than 40 wt.% PES always remain amorphous upon cooling. The crystallisation peak of the 75/25 PEO/PES blend also shifts to lower temperatures with increasing homogenisation

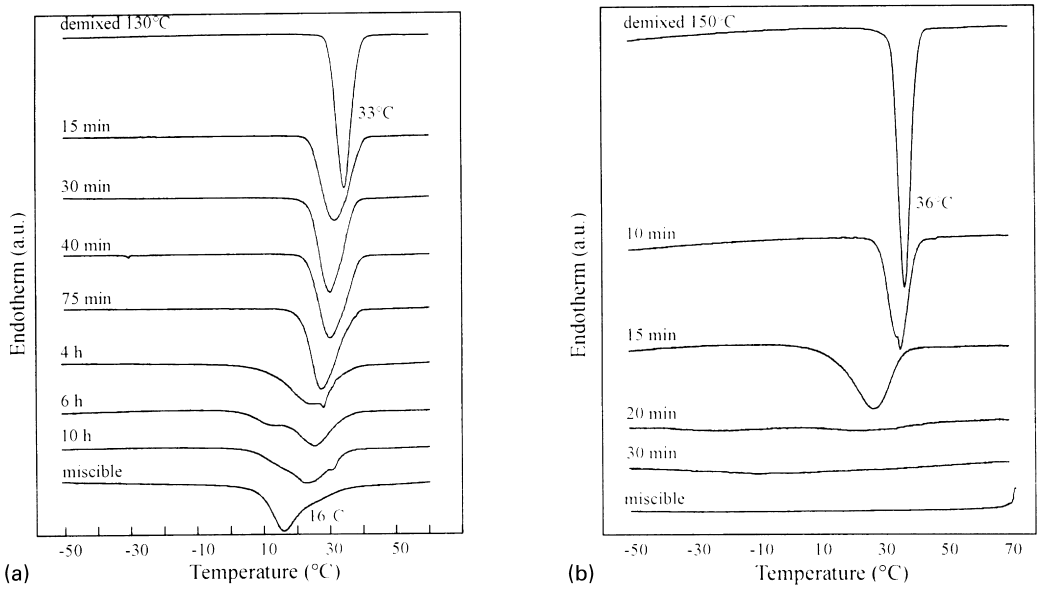


Fig. 4. DSC cooling curves of: (a) 75/25 PEO/PES blends demixed for 15 min at 130°C, remixing at 70°C and (b) 50/50 PEO/PES blends demixed for 15 min at 150°C, remixing at 90°C after different remixing times (indicated left of the curve).

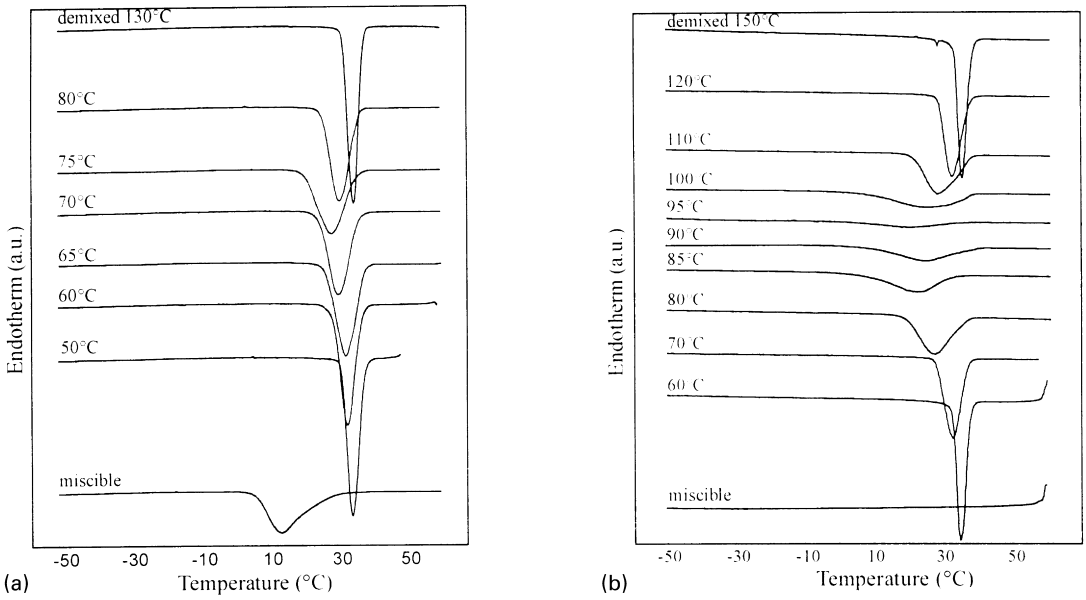


Fig. 5. DSC cooling curves of: (a) 75/25 PEO/PES blends demixed for 5 min at 130°C and (b) 50/50 PEO/PES blends demixed for 5 min at 150°C, after remixing for 10 min at different temperatures (indicated left of the curve).

time. Again, the process proceeds on the molecular level but complete remixing does not appear within 10 h. In this case, a small difference in crystallisation temperatures of this blend compared to the same blend in the miscible state is still present.

### *3.1.4. Influence of remixing temperature*

The influence of the remixing temperature ($T_r$) on the homogenisation process was investigated after demixing the 75/25 and 50/50 PEO/PES blends for 5 min at 130 and 150°C, respectively. The DSC-traces of blends remixed at various temperatures for 10 min are given in Fig. 5. From $T_r = 120$°C to $T_r = 95$°C, the 50/50 PEO/PES blend shows a decrease in crystallisation temperature indicating an increasing level of homogenisation. By contrast, from $T_r = 95$°C to $T_r = 60$°C the crystallisation temperature increases indicating that remixing slows down with decreasing temperature. Similar behaviour is observed for the 75/25 PEO/PES blend with a maximum remixing rate at 75°C. The crystallinity decreases strongly after the homogenisation process as presented in Table 1.

Firstly, within the miscible temperature/composition region of the phase diagram, the remixing process slows down with decreasing temperature due to the lower mobility of the PEO and PES chains. The homogenisation process is diffusion-controlled and shows strong temperature

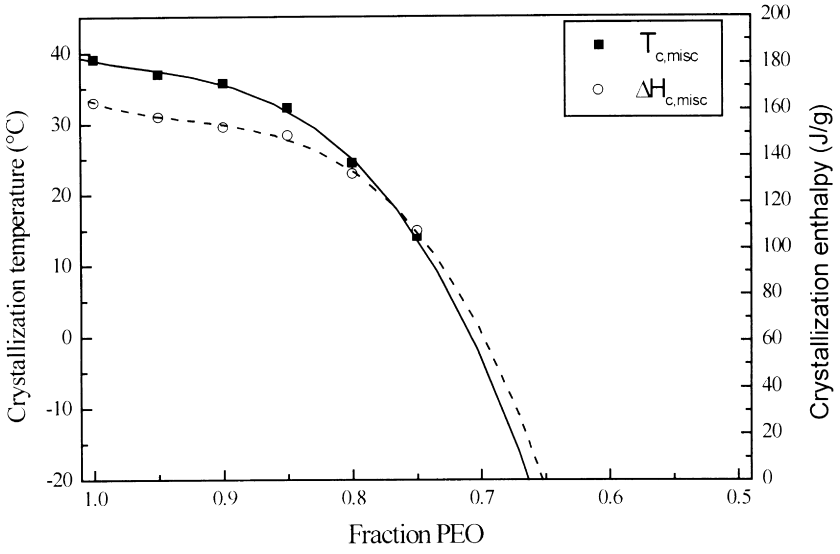


Fig. 6. Crystallisation temperature ($T_{c,misc}$) and crystallisation enthalpy ($\Delta H_{c,misc}$) of PEO/PES blends in the miscible state as a function of the fraction PEO.

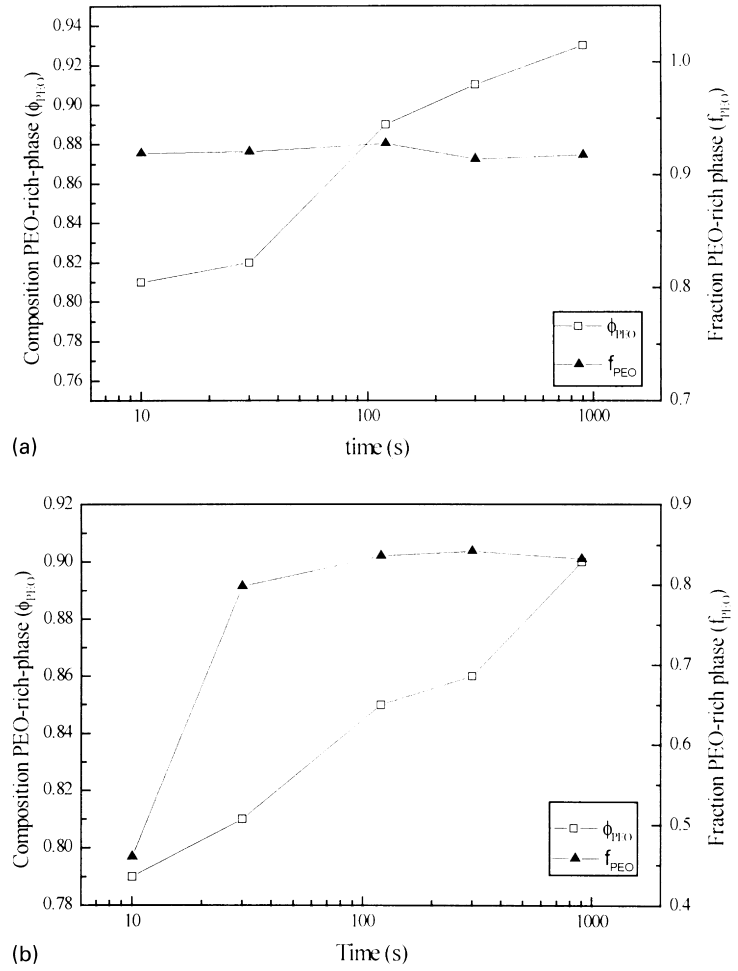


Fig. 7. (□) Composition of the PEO-rich phase ($\varphi_{PEO}$) and (▲) fraction of the PEO-rich phase ($f_{PEO}$) versus logarithm of demixing time of: (a) 75/25 PEO/PES blend at 130°C and (b) 50/50 PEO/PES blend at 150°C.

dependency. Secondly, above the cloud point temperature homogenisation is only partially possible and the process is thermodynamically controlled. The extent of remixing depends on the Gibbs free energy gain of the partially demixed system, which decreases with increasing temperature.

*3.1.5. Determination of the composition and amount of the PEO-rich phase in the partially phase separated blends*

The drastic variation of the crystallisation temperature and crystallisation enthalpy with increasing amount of amorphous component in the blends considered, allows us to estimate the amount of the PEO-rich phase ($f_{PEO}$) as well as the concentration of PEO in this phase ($\varphi_{PEO}$).

From dynamic crystallisation of PEO/PES blends in the miscible state the crystallisation temperature ($T_{c,misc}$) and the crystallisation enthalpy ($\Delta H_{c,misc}$) are obtained as a function of the PEO-content as shown in Fig. 6. The dependence of $T_{c,misc}$ on the PEO content is used to estimate the composition of the PEO-rich phase ($\varphi_{PEO}$) from the crystallisation temperature ($T_{c,exp}$) of the phase separated blend. Moreover, the $\Delta H_{c,misc}$ versus fraction PEO curve is used to estimate the fraction of PEO-rich phase ($f_{PEO}$). One proceeds as follows: from $T_{c,exp}$ one obtains the fraction PEO in the PEO-rich phase and this allows us to estimate the crystallisation enthalpy ($\Delta H_{c,misc}$) of a PEO/PES blend in the miscible state with the same composition. The fraction of PEO-rich phase ($f_{PEO}$) in the phase-separated blend is obtained by rationing $\Delta H_{c,misc}$ by the crystallisation enthalpy of the phase-separated blend $\Delta H_{c,exp}$

$$f_{PEO} = \frac{\Delta H_{c,exp}}{\Delta H_{c,misc}}. \quad (4)$$

It is clear that the $\varphi_{PEO}$ of the phase-separated system is always higher than the PEO content of the blend in the miscible state and that $f_{PEO}$ changes from 0 to 1. The change of the described parameters during demixing and remixing is discussed below.

The composition of the PEO-rich phase ($\varphi_{PEO}$) and the fraction of PEO-rich phase ($f_{PEO}$) as a function of demixing time are presented in Fig. 7. The demixing conditions are the following: 75/25 PEO/PES blend, $T_d = 130$°C and 50/50 PEO/PES blend, $T_d = 150$°C. The 50/50 PEO/PES blend

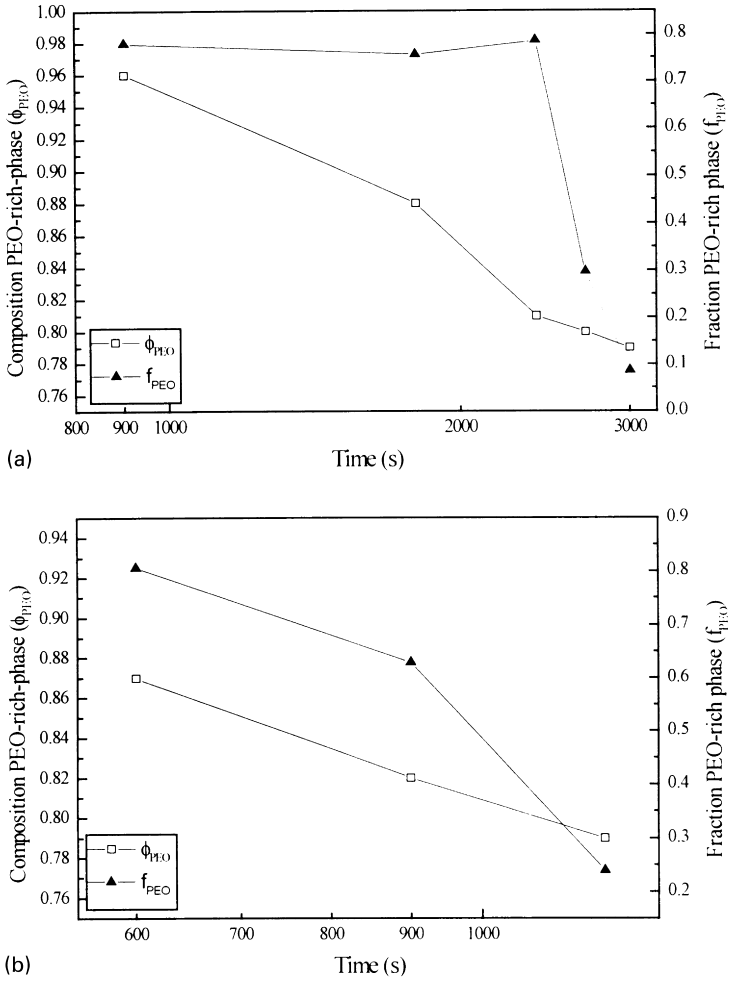


Fig. 8. (□) Composition of the PEO-rich phase ($\varphi_{PEO}$) and (▲) fraction of the PEO-rich phase ($f_{PEO}$) versus logarithm of remixing time of the 50/50 PEO/PES blend phase separated for 5 min at 150°C, during remixing at: (a) 70°C and (b) 90°C.

shows an almost linear relation between $\varphi_{PEO}$ and the logarithm of time; $\varphi_{PEO}$ changes from 0.79 after 10 s to 0.90 after 15 min demixing. $f_{PEO}$ rapidly increases at short demixing times and stabilises at 0.84. The 75/25 PEO/PES blend displays similar changes: $\varphi_{PEO}$ changes monotonically, while $f_{PEO}$ is found constant at 0.9. Clearly, the phase separation process consists of two different processes: appearance of concentration fluctuations and evolution of the amplitude of these fluctuations. From the analysis of $\varphi_{PEO}$ and $f_{PEO,}$ it becomes clear that structure formation is completed while the composition of the co-existing phases still changes. This agrees with the Cahn–Hilliard theory proposed for spinodal phase separation [26,27]. In accordance with this theory, the wavelength of the concentration fluctuation is constant during the early and intermediate stages of spinodal decomposition and only the amplitude of the concentration fluctuation changes. The wavelength of the concentration fluctuation corresponds in this case to the fraction of the PEO-rich phase, $f_{PEO}$. It is constant for the 75/25 PEO/PES blend and levels out almost instantly (within 30 s) for the 50/50 PEO/PES blend. The somewhat lower value found after 10 s might be related to the insufficient sensitivity of the DSC to weak and broad signals. $\varphi_{PEO}$ corresponds to the amplitude of the concentration fluctuation and changes continuously as predicted by the model.

The evolution of the composition and fraction of the PEO-rich phase during remixing at 70 and 90°C of a 50/50 PEO/PES blend, initially demixed for 15 min at 150°C, are presented in Fig. 8. At both remixing temperatures, a monotonic decrease of $\varphi_{PEO}$ with the logarithm of time is observed. In addition, $f_{PEO}$ remains constant at 70°C for 45 min, whereas at 90°C it decreases already after 15 min This is in agreement with light scattering experiments performed by Inoue et al. during homogenisation of a spinodal demixed system [28], which proceeds in two steps. Firstly, mutual diffusion of PEO and PES chains changes the composition of both phases (the amplitude of the concentration fluctuation) whereas the volume fraction of these phases (the wavelength of the concentration fluctuation) remains nearly constant. Secondly, the value of $f_{PEO}$ decreases. The homogenisation process of partially phase separated polymer blends proceeds in the order reversed

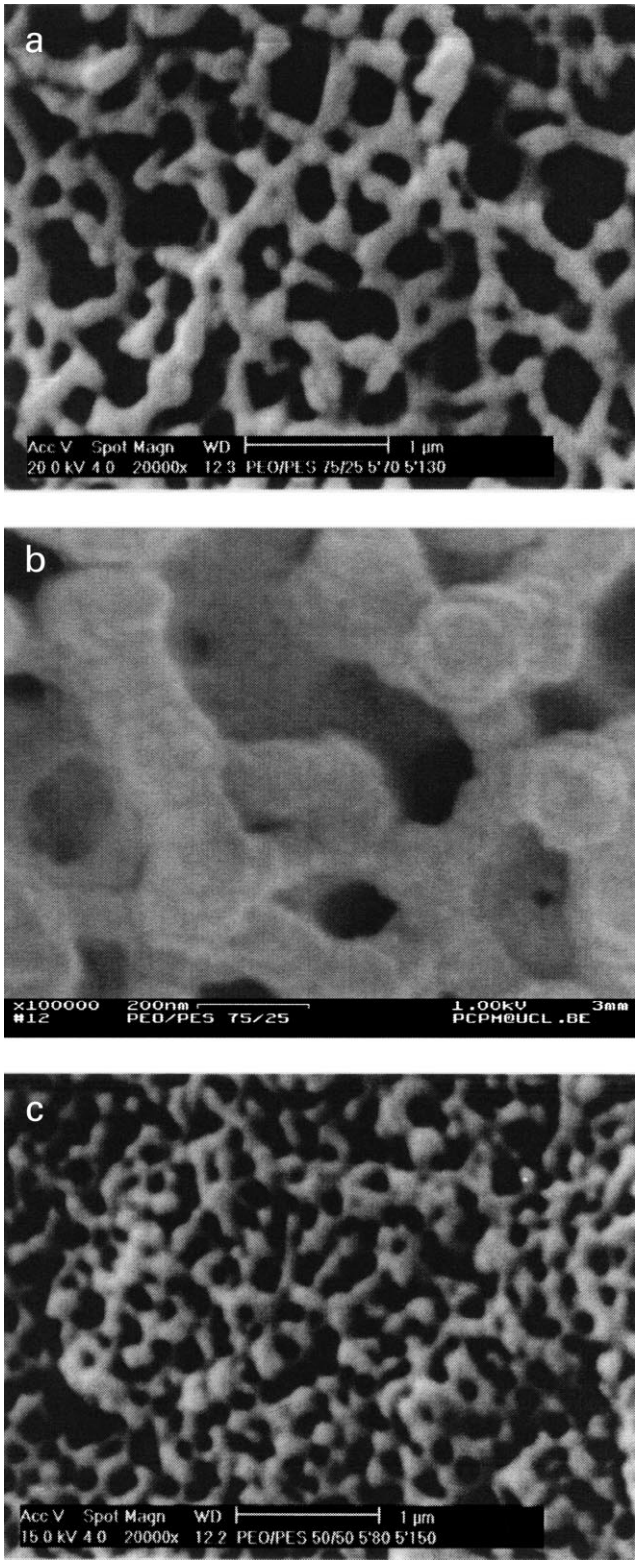


Fig. 9. SEM-pictures after phase separation and crystallisation of: (a) and (b) 75/25 PEO/PES blend phase separated for 5 min at 130°C and (c) 50/50 PEO/PES blend phase separated 5 min at 150°C. Etching time 3 h.

with respect to the phase separation; initially the concentration difference between both phases decreases and finally the phase structure disintegrates.

### 3.2. Phase morphology of demixed PEO/PES blends

The DSC-study of the evolution of the composition and amount of PEO-rich phase in the phase separated blends revealed that the phase separation process is of the spinodal type; this signifies that a co-continuous structure is formed. This will be described in the following section.

The phase morphology of 75/25 and 50/50 PEO/PES blends was investigated by means of scanning electron microscopy and atomic force microscopy. Solvent etching for 3 h removed the PEO-rich phase from the phase-separated blends. SEM-pictures of a 75/25 and a 50/50 PEO/PES blend initially demixed for 5 min at 130 and 150°C, respectively, and dynamically crystallised are shown in Fig. 9.

75/25 and 50/50 PEO/PES blends (Fig.9(a)–(c)) show a clear co-continuous structure, in accordance with the DSC-results, with a characteristic dimension of approximately 400 and 200 nm, respectively. At higher magnification (Fig. 9(b)), FEG-SEM enables a more detailed observation of this morphology. The small grains with diameter of about 30–40 nm present in the picture can be attributed to the rough structure typically observed on sputtered gold films and are an artefact of the sample preparation.

However, despite the relatively high lateral resolution achieved with electron microscopy, it is not possible to examine the semi-crystalline structure of the samples using SEM. The inability of the electron microscopy to resolve the semi-crystalline features can be related to an insufficient depth of focus. In addition, the presence of the gold layer with a thickness of 50 nm (verified by AFM), which is larger than the long periodicity of the semi-crystalline structure, can smear out the crystalline features. Therefore, a series of AFM measurements were performed on PEO/PES samples, without gold coating. The samples were etched for only 12 min in order to keep the PEO-rich phase close to the surface and etch away only amorphous PEO material present on the surface. A SEM-image of a 75/25 PEO/PES blend (5 min demixing 130°C) shows a typical surface morphology obtained under these conditions (Fig. 10(a)). Only the phase morphology can be resolved in this figure. A typical AFM topographic image of the same sample of the demixed 75/25 PEO/PES blend is presented in Fig. 10(b). In this image, many facetted entities are observed. These entities form terraces with rather flat surfaces and are organised in stacks. They can be attributed to the PEO lamellar crystals. Apart from these features, some disordered globular morphology with a size close to that of the phase-separated structure visualised by SEM appears. Less facetted entities are found in the case of the 50/50 PEO/PES blend (Fig. 11) in agreement with the lower PEO content in this blend. The AFM topographical image (Fig. 11(a)) shows the presence of some crystalline features

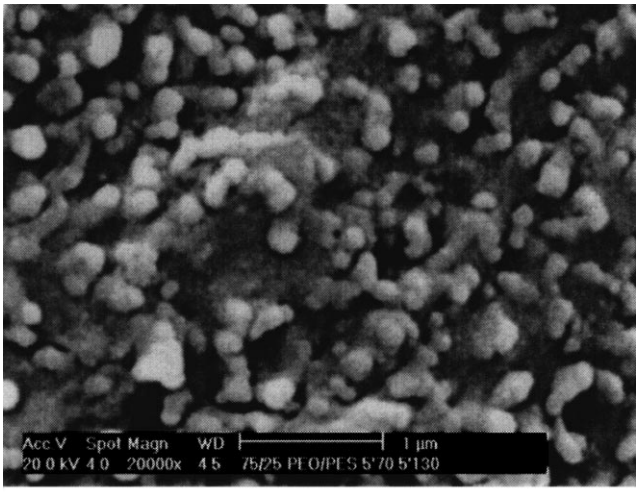


(a)

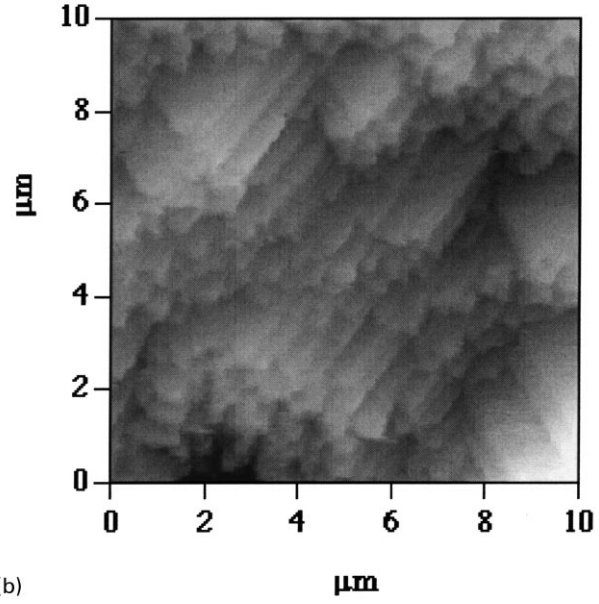


(b)

Fig. 10. 75/25 PEO/PES blend phase separated for 5 min at 130°C and subsequently dynamically crystallised: (a) SEM-pictures and (b) AFM topographic image. Etching time 12 min.

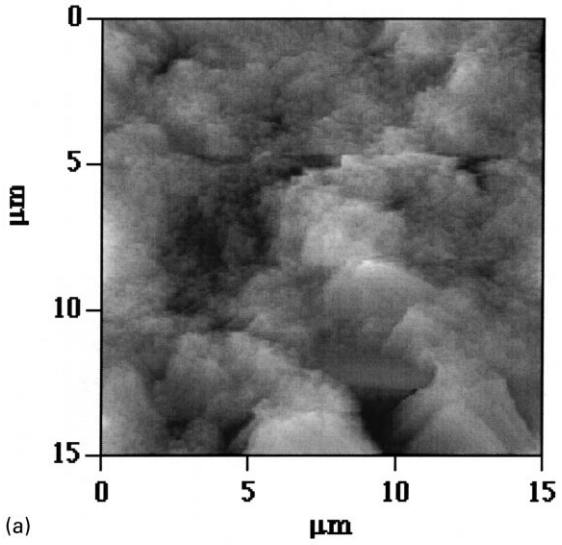


(a)

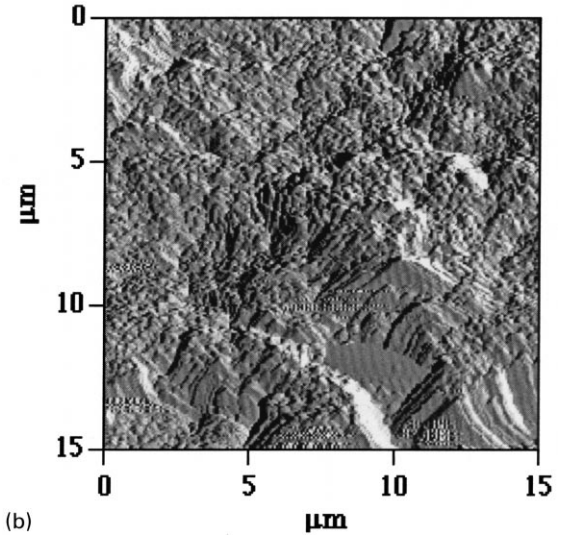


(b)

Fig. 11. 50/50 PEO/PES blend phase separated for 5 min at 150°C and subsequently dynamically crystallised: (a) AFM topographic image and (b) deflection image of the same sample. Etching time 12 min.

(bottom of the figure) together with the disordered morphology. The crystalline structure appears more pronounced in the corresponding deflection image (Fig. 11(b)). In order to quantify the AFM observations, the angle between the crystal facets taking into account the longitudinal and lateral inclinations of basal crystal planes was calculated. The obtained values of about 70–77° are less than expected for crystals with the (120) growth face that reveal almost rectangular shape [29]. In addition, the occurrence of curved crystal edges (low right corner of Fig. 11(b)) can be due to the change in the folding direction during crystallisation, as temperature decreases [30]. Scanning electron and atomic force microscopy provide complementary information with respect to the morphology of PEO/PES blends. While SEM allows us to analyse the details of the phase separated structure, AFM reveals the semi-crystalline morphology and, in particular, the shape of the PEO crystals.

### *3.3. Semi-crystalline morphology of demixed PEO/PES blends*

It became clear that phase separation of PEO/PES blends generates a co-continuous nano-structure in which the crystallisation behaviour strongly differs from that of the miscible state. AFM revealed that lamellar crystalline structures of PEO are present in the phase-separated structure. The semi-crystalline morphology of the phase separated PEO/PES blends is discussed below.

Real-time small angle and wide angle X-ray scattering (SAXS and WAXD) were performed during the phase separation and crystallisation of PEO/PES blends.

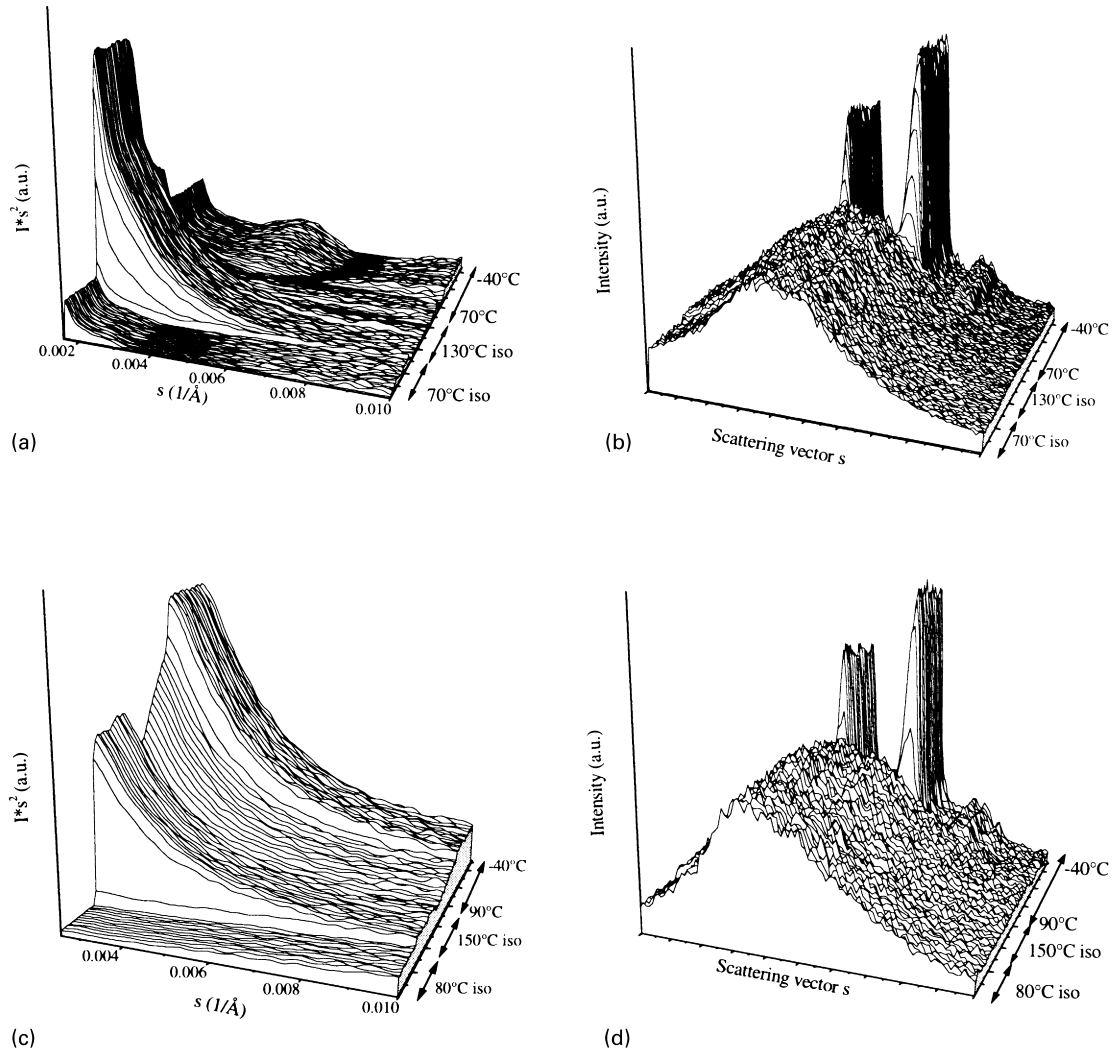


Fig. 12. Lorent-corrected SAXS-patterns and WAXD patterns during phase separation and crystallisation of: (a) and (b) 75/25 PEO/PES blend, (c) and (d) 50/50 PEO/PES blend. The temperature profile is presented in Fig. 13.

Lorentz-corrected SAXS profiles and WAXD curves of a 75/25 and a 50/50 PEO/PES blend during melting, isothermal demixing and subsequent crystallisation are presented in Fig. 12. The temperature program used in these experiments is shown together with the evolution of the SAXS invariant, *Q*, in Fig. 13.

The SAXS-profile of the 75/25 PEO/PES blend (Fig. 12(a)) reveals a strong increase of the scattered intensity at small values of *s* when the system demixes at 130°C. During cooling a scattering maximum in the SAXS-profile and crystalline diffraction peaks in the WAXD-patterns appear. These changes occur around 35°C as can be seen from the scattering invariant (Fig. 13(a)). The 50/50 PEO/PES blend displays a similar increase of the scattering intensity at small angles when phase separation occurs at 150°C (Fig. 12(c)). Upon cooling, an increase of the scattering invariant (Fig. 13(b)) around 35°C is detected and diffraction peaks appear simultaneously in the WAXD-profiles (Fig. 12(d)). However, in the latter case no scattering maximum is detected in the Lorentz corrected SAXS-curves.

The increase of the scattering behaviour upon phase separation can be related to the formation of a two-phase system characterised by different electron densities. As the characteristic domain size of the phase morphology is beyond the *s*-range probed by SAXS, no maximum is observed. On the contrary, the crystallisation of PEO generates a maximum in the SAXS-patterns of the 75/25 PEO/PES blend that arises from the repetition distance within PEO lamellar stacks. This maximum corresponds to a long period of 210 Å. SAXS patterns of the demixed and remixed 50/50 PEO/PES blends were investigated in more detail and in any case a maximum was observed upon crystallisation. Since, the 50/50 PEO/PES blend shows WAXD patterns with scattering peaks at the same positions as pure PEO (0.22 and 0.26 $Å^{-1}$), the crystalline unit cell remains unchanged. The absence of a SAXS maximum for the 50/50 PEO/PES blend together with the wide-angle diffraction

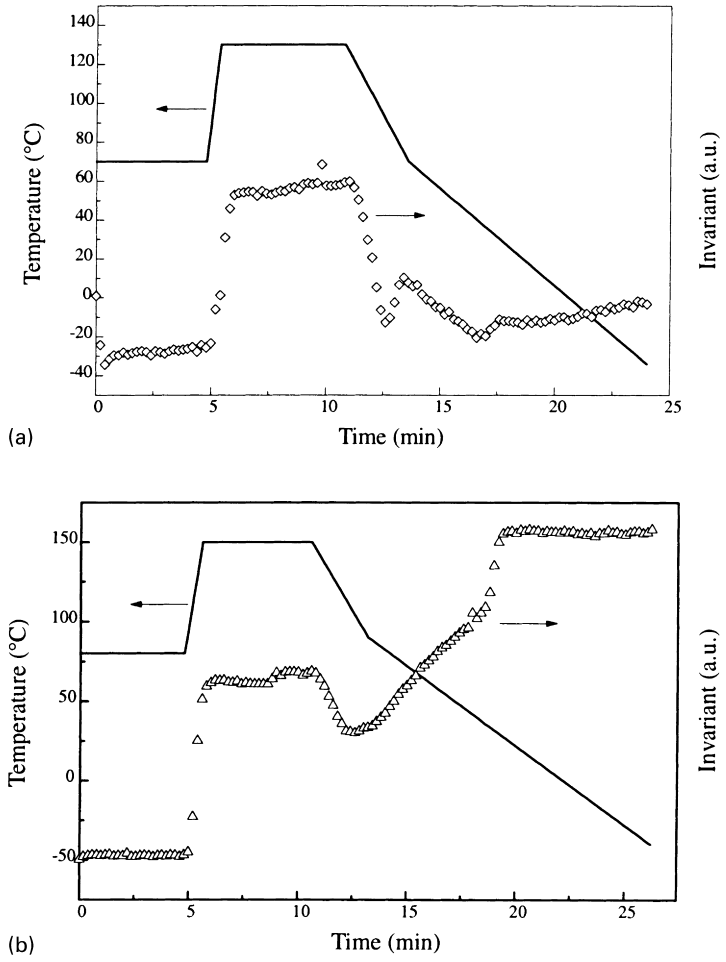


Fig. 13. Applied temperature profile and SAXS scattering invariant *Q* during separation and crystallisation of: (a) 75/25 PEO/PES blend and (b) 50/50 PEO/PES blend.

pattern indicates that a different semi-crystalline structure is formed in this blend.

The crystalline structure of a 75/25 PEO/PES blend demixed for 5 min at 130°C and that of a 50/50 PEO/PES blend demixed for 5 min at 150°C observed with polarised optical microscopy are presented in Fig. 14. The 75/25 PEO/PES blend shows the occurrence of classical Maltese crosses indicating the presence of a spherulitic superstructure. Although the 50/50 PEO/PES blend shows some birefringence, no Maltese crosses appear. The observed birefringence of the partially demixed 50/50 PEO/PES blend in combination with the crystalline structures observed by AFM indicate that PEO lamellae are present but not organised in a spherulitic superstructure.

The difference between the semi-crystalline morphology of the 75/25 and the 50/50 PEO/PES blends in the demixed state can be conceived from the amount and the dimensions of the PEO-rich phase. The characteristic dimensions are larger in a 75/25 blend than in a phase-separated 50/50 PEO/PES blend which facilitates spherulitic growth.

## 4. Conclusions

The crystallisation behaviour of phase-separated PEO/PES blends strongly depends on the demixing temperature and time. The two-phase system formed during the phase separation process contains one phase with a higher amount of the crystallizable component PEO and crystallises faster than the initial PEO/PES blend in the miscible state.

The composition and fraction of the PEO-rich phase in the phase-separated blends is obtained from the dynamic crystallisation behaviour. The evolution of these parameters during an isothermal demixing process corresponds to spinodal decomposition and validates the proposed method. The applicability of this method concerns mainly partially miscible crystalline/amorphous blends possessing a sufficiently large difference in crystallisation temperature and crystallisation enthalpy between the miscible and phase separated state.

The observed phase morphology of the phase-separated blends presents a co-continuous structure with nanometer dimensions and is the result of spinodal demixing. The

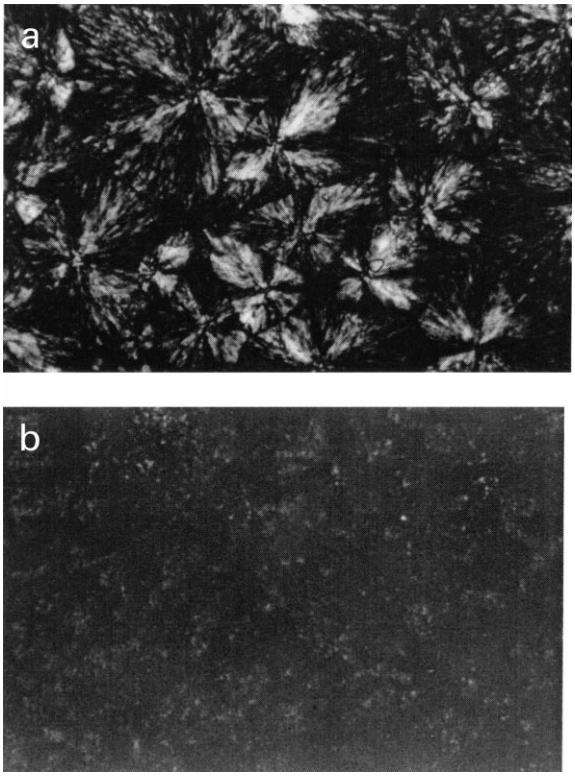


Fig. 14. Polarised optical micrographs after phase separation and crystallisation of: (a) 75/25 PEO/PES blend demixed for 5 min at 130°C and (b) 50/50 PEO/PES blend demixed for 5 min at 150°C (magnification: 300 times).

facets of PEO crystalline lamellae could be visualised in these systems by AFM. Time-resolved small angle X-ray scattering experiments reveal that lamellar stacks are not necessarily present for all crystalline blends. Apparently, the occurrence of lamellar stacks in phase separated PEO/PES blends is related to the formation of a spherulitic superstructure and can be explained from the characteristic size of the phase structures.

## Acknowledgements

This research was financially supported by the Research Council, Catholic University of Leuven and the Fund for Scientific Research Flanders (FWO-Vlaanderen). One of the authors (G. Dreezen) is indebted to the Flemish Institute for the promotion of Scientific-Technological Research in Industry (I.W.T.) for a fellowship. We thank Prof H. Reynaers (Catholic University of Leuven) and Dr M. Koch (EMBL), as well as the European Union for support of the work at EMBL, Hamburg, Germany, through the HCMP Access to Large Installations Project, Contract Number CHGE-CT93-0040.

## References

[1] Tanaka H, Nishi T. Phys Rev Lett 1985;55(10):1102.
[2] Tanaka H, Nishi T. Phys Rev A 1989;39(2):783.
[3] Li Y, Stein M, Jungnickel B-J. Colloid Polym Sci 1991;269:772.
[4] Li Y, Schneider L, Jungnickel B-J. Polym Networks Blends 1992;2(3):135.
[5] Delimoy D, Goffaux B, Devaux J, Legras R. Polymer 1995;36(17):3255.
[6] Inaba N, Yamada T, Suzuki S, Hashimoto T. Macromolecules 1988;21:407.
[7] Schulze K, Kressler J, Kammer H. Polymer 1993;34:3704.
[8] Cham PM, Lee TH, Marand H. Macromolecules 1994;27:4263.
[9] Okamoto M, Inoue T. Polymer 1995;36(14):2739.
[10] Shibanov Y, Godovsky Y. Progr Colloid Polym Sci 1989;80:110.
[11] Shibanov Y, Godovsky Y. Makromol Chem, Macromol Symp 1991;44:61.
[12] Li Y, Jungnickel B-J. Polymer 1993;34:9.
[13] Wellscheid R, Wüst J, Jungnickel B-J. J Polym Sci: B Polym Phys 1996;34:267.
[14] Walsh D, Singh V. Makromol Chem 1984;185:1979.
[15] Guo W, Higgins J. Polymer 1990;31:699.
[16] Walsh D, Rostami S, Singh V. Makromol Chem 1985;186:145.
[17] Dreezen G, Fang Z, Groeninckx G. Polymer 1999; in press.
[18] Dreezen G, Mischenko N, Koch MHJ, Reynaers H, Groeninckx G. Macromolecules; in press.
[19] Gaur U, Lau SF, Shu HC, Wunderlich BB. J Phys Chem Ref Data, 10, (1981) 89,119 1001;11 (1982) 313, 1065; 12, (1983) 29;65;91.
[20] Varma-Nair M, Wunderlich BB, Mehta A. J Phys Chem Ref Data 1991;20(2):349.
[21] Koch MHJ, Bordas J. Nucl Instrum Meth 1983;208:461.
[22] Boulin CJ, Kempf R, Gabriel A, Koch MHJ. Nucl Instrum Meth 1988;A269:312.
[23] Crist B, Morosoff N. J Appl Polym Sci: Polym Phys Ed 1973;11:1023.
[24] Bu HS, Cheng SZD, Wunderlich B. Polym Bull 1987;17:567.
[25] Fox TG. Bull Am Phys Soc 1956;2:1123.
[26] Cahn JW, Hilliard JE. J Chem Phys 1958;28:285.
[27] Thermodynamics and kinetics of phase separation. In: Klempner D, Sperling H, Utracki LA, editors. Interpenetrating polymer networks, Washington, DC: American Chemical Society, 1994. pp. 78 Chapter 3.
[28] Okamoto M, Shiomi K, Inoue T. Polymer 1995;36:87.
[29] Snétivy D, Vancso GJ. Polymer 1992;33:432.
[30] Marentette JM, Brown GR. Polymer 1998;39:1405.